The stellar content of UCHII regions: the molecular cloud GRSMC 045.49+00.05

N. Azatyan *[1], E. Nikoghosyan[1], L. Kaper[2], D. Andreasyan[1], A. Samsonyan[1], A. Yeghikyan[1], D. Baghdasaryan[1], and N. Harutyunyan[3]

[1]Byurakan Astrophysical Observatory, 0213 Aragatsotn Prov., Armenia
[2]Anton Pannekoek Institute for Astronomy, University of Amsterdam,, Science Park 904, 1098 XH Amsterdam, The Netherlands
[2]Department of Physics, Yerevan State University, 1 Alex Manoogian st.,, 0025, Yerevan, Armenia,

Abstract

Ultra-compact H II (UC HII) regions are an important phase in the formation and early evolution of massive stars. The main objectives of this work are to study the stellar content associated with the G045.49+00.04 and G045.14+00.14 star-forming regions located in the GRSMC 45.46+0.05 molecular cloud at a distance of about 8 kpc. Both regions contain a number of UC HII regions. The main objective is to characterize the embedded young stellar objects (YSOs), such as their mass, evolutionary age and age spread, spatial distribution, luminosity function. We used near-, mid-, and far-infrared photometric data to identify and classify the YSOs. Their main parameters were determined by the spectral energy distribution (SED) fitting tool using radiation transfer models. Totally, we identified 2864 YSOs. We also constructed a colour-magnitude diagram to compare the parameters of stellar objects with the results of the radiative transfer models. The density distribution of the identified YSOs showed the presence of dense clusters in the UC HII regions. The parameters of YSOs in the IRAS clusters and non-cluster objects surrounding them show some differences. In general, the YSOs in these clusters have an evolutionary age larger than 10^6 years with an age spread of a few Myr. The clusters include several high- and intermediate-mass zero-age main sequence stellar objects. The small age spread suggests that the clusters may originate from a single triggering event.

Keywords: *stars: pre-main sequence – Stars: luminosity function – Infrared: stars – radiative transfer*

1. Introduction

Massive stars are generally recognised to form inside dense ($n > 10^3$ cm^{-3}) and cold (T ∼10–30 K) compact clumps in giant molecular clouds (GMCs) (e.g. Lada & Lada, 2003). Based on results obtained for different massive star-forming regions, star formation in these clumps appears to be triggered by compression from external shocks. If star formation is triggered by compression, the age spread of the new generation of stars should be small (Zinnecker et al., 1993).

Massive stars and the star clusters hosting them are thought to play an important role in the evolution of galaxies. They affect their environment by shaping the morphology, energy, and chemistry of the interstellar medium (ISM) through phenomena such as outflows, stellar winds, and supernovae (McKee & Tan, 2003). The energy injected into the surrounding neutral ISM may trigger the formation of new stars (Elmegreen & Lada, 1977).

The main challenges in studying high-mass star formation include: (i) the newly formed massive stars are deeply embedded in GMCs, (ii) massive stars are rare, and (iii) they begin burning their nuclear fuel, i.e. reach the zero-age main sequence (ZAMS) while still accreting (McKee & Tan, 2003, Peters et al., 2010). Understanding the formation and early evolution of massive stars requires detailed knowledge of the environments where star-forming events occur. Massive stars produce powerful Lyman continuum emission that is sufficiently energetic to ionise their surroundings and create observable ionised H II regions (Churchwell, 2002, Keto, 2007). Thus, UC HII regions are the sites of the early stages of massive star formation. These represent ideal natural laboratories to investigate the influence of hot massive stars on their environment.

*nayazatyan@bao.sci.am, Corresponding author

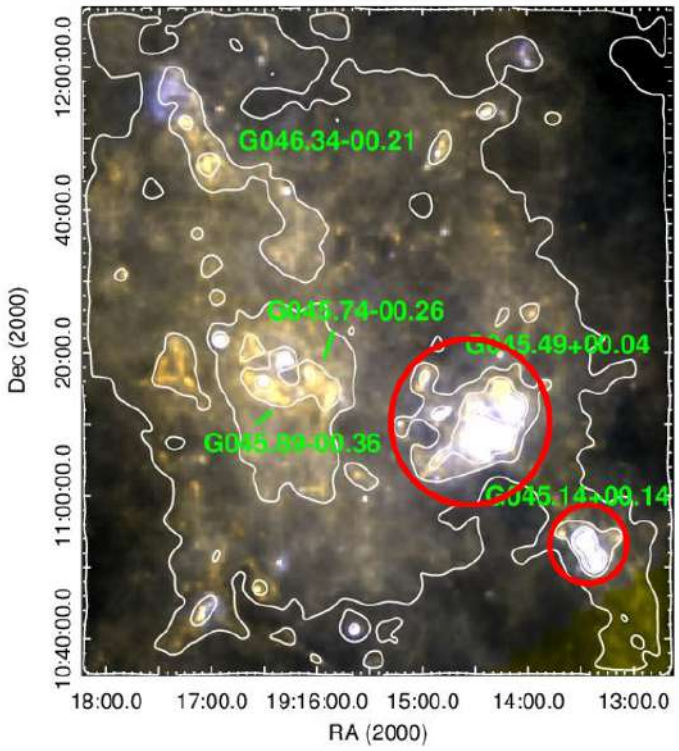

Figure 1. Colour-composite *Herschel* images of GRSMC 45.46+0.05 molecular cloud: 160 μm (blue), 350 μm (green), and 500 μm (red) bands. G045.49+00.04 and G045.14+00.14 star-forming regions are mentioned with red circles.

The main goal of this work is the study of stellar content in G045.49+00.04 and G045.14+00.14 star-forming regions which are part of the Galactic Ring Survey Molecular Cloud (GRSMC) 45.46+0.05 large star formation complex (Simon et al., 2001) at a distance of about 8 kpc (e.g., Wu et al., 2019). This complex is an ideal laboratory to investigate the early stages of massive star formations and their influence on natal environments since it contains a number of H II. Figure 1 shows G045.49+00.04 and G045.14+00.14 star-forming regions by red circles. Both regions also contain UC HIIs. The regions are sites of active star formation and have a complex hierarchical structure, containing a large number of high-mass stars at different stages of evolution. Based on data of stellar groups composition and putative triggers of star formation, we will be able to reconstruct the history of star formation in the regions.

In this paper, we present the results of a near-, mid-, and far-infrared (NIR, MIR, and FIR) study of the UC HIIs in G045.49+00.04 and G045.14+00.14 star-forming regions. We aim to better understand (i) the physical properties of dense molecular and ionised gas in the immediate neighbourhood of UC HII regions; (ii) the properties of embedded massive stars or star clusters; and (iii) whether the formation of the embedded massive stars or star clusters was triggered.

We have organised the paper as follows. Section 2 describes the used data; in Section 3 we present the methods; in Section 4, we analyse the stellar population in the regions. Finally, the study results are summarised in Section 5.

2. Used data

We used data covering a wide range of NIR to FIR wavelengths. The first database is the archival NIR photometric data in the J, H, and K bands of the Galactic Plane Survey DR6 (UKIDSS GPS, Lucas et al., 2008) with a resolution of 0.1″/px. This survey is complete to approximately 18 mag in the K band and provides a percentage probability of an individual object being a star, galaxy, or noise.

Archival MIR observations were obtained from the Galactic Legacy Infrared Midplane Survey Extraordinaire (GLIMPSE, Churchwell et al., 2009), using the *Spitzer* Infrared Array Camera (IRAC, Fazio et al., 2004). The four IRAC bands are centred at approximately 3.6, 4.5, 5.8, and 8.0 μm with a resolution of 0.6″/px. At longer wavelengths, we used data from a survey of the inner Galactic plane using the Multiband Infrared Photometer for *Spitzer* (MIPSGAL). We also used Wide-field Infrared Survey Explorer (WISE,

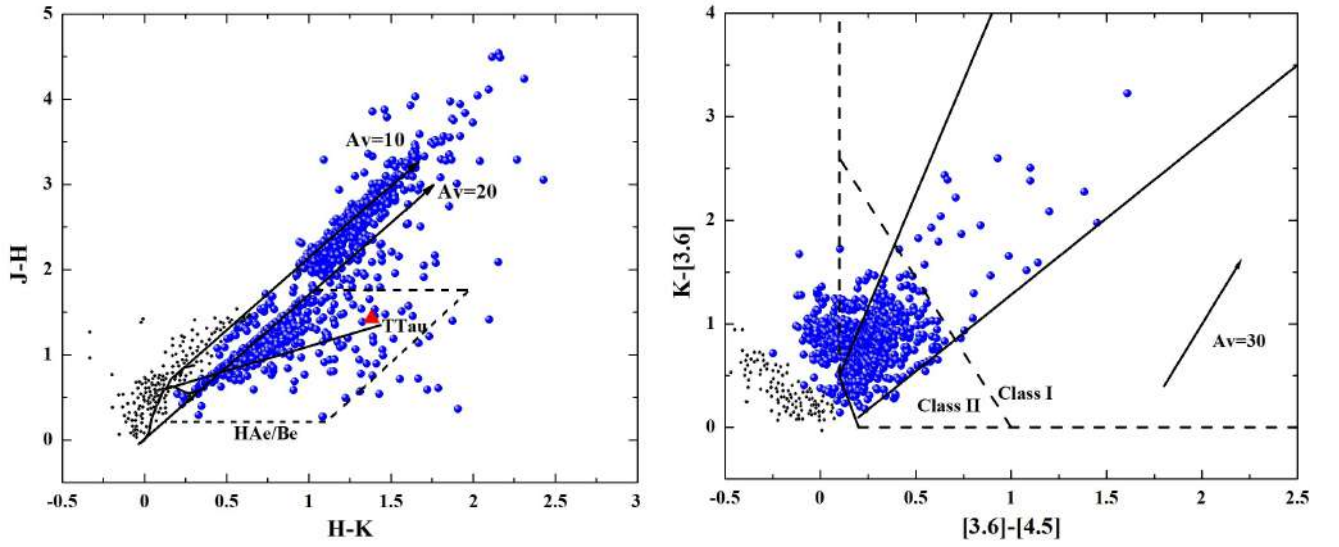

Figure 2. Two colour-colour diagrams of the G045.14+00.14 star-forming region. *Left panel*: (J-H) vs. (H-K) diagram. *Right panel*: K-[3.6] vs. [3.6]-[4.5] diagram. The blue circles are selected YSO candidates and black circles are non-classified ones. Not all non-classified objects are presented in these diagrams. IRAS 19111+1048 source is indicated by a red triangle.

Wright et al., 2010) data in the 3.4, 4.6, 12, and 22 μm bandpasses.

To study deeply embedded point sources, we used FIR observations, in the 70–500 μm range, obtained with the Photodetector Array Camera and Spectrometer (PACS, Poglitsch et al., 2010) and the Spectral and Photometric Imaging Receiver (SPIRE, Griffin et al., 2010) on board the 3.5 m *Herschel* Space Observatory (Pilbratt et al., 2010). For our analyses, we used photometric data and images from the PACS 70 and 160 μm catalogues, in addition to *Herschel* infrared Galactic Plane Survey (Hi-GAL, Molinari et al., 2016) data at 70, 160, 250, 350, and 500 μm.

3. Methods

The identification of stellar objects was performed with GPS UKIDSS-DR6 as the main catalogue, and then other MIR and FIR catalogues were cross-matched with it within 3 σ of the combined error–matching radius. The GPS UKIDSS-DR6 catalogue provides the probability of an object being a star, galaxy, or noise based on its image profile. The UKIDSS team recommends that sources classified as noise should be excluded since most of them are not real sources (Lucas et al., 2008). We selected objects with a $< 30\,\%$ probability of being noise and a magnitude of $K < 18.02$ mag, taking into account the K band limit of the UKIDSS survey. In addition, we removed objects with zero errors of measured magnitudes in the J, H, and K bands. This yielded a total of approximately 134,000 objects.

One of the main observational characteristics of YSOs is an IR excess due to the presence of circumstellar discs and envelopes (Hartmann, 2009, Lada & Lada, 2003); furthermore, the measure of the IR excess in the NIR and/or MIR ranges can be used to characterise the evolutionary stage of a YSO (Class I and Class II). YSO candidates can be identified based on their position in colour–colour (c-c) diagrams. To confirm the selected YSOs and to determine their parameters, we constructed their SEDs and fitted them with the radiative transfer models of (Robitaille et al., 2007).

4. Results

Since c-c diagrams are useful tools to identify YSO candidates, we constructed six c-c diagrams, namely (J-H) vs. (H-K), K-[3.6] vs. [3.6]-[4.5], [3.6]-[4.5] vs. [5.8]-[8.0], [3.6]-[5.8] vs. [8.0]-[24], [3.4]-[4.6] vs. [4.6]-[12] and [3.4]-[4.6] vs. [4.6]-[22]. Figure 2 shows only two c-c diagrams of G045.14+00.14 star-forming region. The same approach has previously been successfully applied to other star-forming region (Azatyan, 2019, Azatyan et al., 2022).

The left panel of Figure 2 shows the (J-H) versus (H-K) c-c diagram and the distribution of objects.

doi:https://doi.org/10.52526/25792776-22.69.2-217

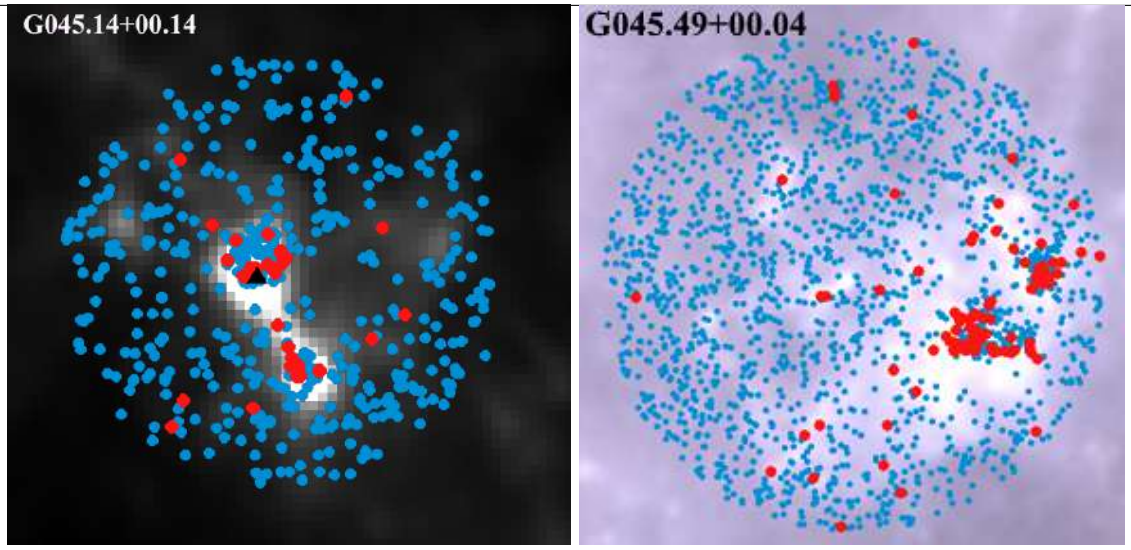

Figure 3. Distribution of YSOs in G045.14+00.14 *(left panel)* and G045.49+00.04 *(light panel)* regions on *Herschel* 500 μm images. Class I and Class II objects are indicated by filled red and blue circles, respectively. IRAS 19111+1048 source is indicated by a black triangle.

The solid and dashed curves represent the loci of the intrinsic colours of dwarf and giant stars (Bessell & Brett, 1988) converted to the CIT system (Carpenter, 2001); the parallel solid lines drawn from the base and tip of these loci are the interstellar reddening vectors (Rieke & Lebofsky, 1985). The locus of unreddened classical T Tauri stars (CTTSs) is taken from Meyer et al. (1997). The region where the intermediate-mass PMS stars, i.e. Herbig Ae/Be stars, are usually found is bounded by dashed lines (Hernández et al., 2005). Objects located to the right of the reddening vectors can be considered YSO candidates, since deviation from the MS and the presence of IR excess can be caused by the existence of a circumstellar disc and envelope. Among the objects located in the reddening band of MS and giants, we classified those that have a (J-K) > 3 mag colour index as Class I evolutionary stage YSOs (Lada & Adams, 1992). These are located in the upper right corner of the diagram.

The other example of our used c-c diagrams is K-[3.6] versus [3.6]-[4.5] which used data from the GLIMPSE catalogue to combine NIR and MIR photometry. This diagram is presented in the right panel of Figure 2, where the diagonal lines outline the YSO location region and the dashed line separates the Class I and Class II object domains. The arrow shows the extinction vector (Flaherty et al., 2007). All lines are taken from Gutermuth et al. (2008).

To minimise the likelihood of making an incorrect selection, we selected YSOs on the criterion of being stars classified as objects with IR excess by at least two c-c diagrams. However, since the region has saturated areas in the MIR band around the IRAS objects, this can lead to the potential loss of objects belonging to the molecular cloud. Accordingly, objects within those areas classified as YSOs based on only the NIR c-c diagram were included in the list of candidate YSOs. The selected YSOs are indicated with blue filled circles and non-classified objects - black circles (Figure 2). Totally, in the two parts of the molecular cloud, we identified 5108 YSO candidates with Class I and Class II evolutionary stages.

To confirm the selected YSOs and to determine their parameters, we constructed their SEDs and fitted them with the radiative transfer models of Robitaille et al. (2007). These models assume an accretion scenario in the star formation process, where a central star is surrounded by an accretion disc, an infalling flattened envelope, and the presence of bipolar cavities. We used the command-line version of the SED fitting tool where numerous precomputed models are available. This procedure was performed using wavelengths ranging from 1.1 μm to 500 μm. For the interstellar extinction, we chose an interval of 10–100 mag that would exceed the results obtained by COBE/DIRBE and IRAS/ISSA maps ($A_v = 10 - 50$ mag, Schlegel et al., 1998). The distance interval corresponds to the estimates made in the previous studies (6.5–9.5 kpc, see Introduction).

As we selected YSOs in the MIR–saturated regions using only their J, H, and K magnitudes, constructing their SEDs based on only three photometric data points does not provide a reliable basis for any conclusions (302 YSOs). Excluding these objects, we achieved relatively robust parameters for 2562 of the 4806 selected YSOs with χ^2 <100 that composes 53% of the total number. Overall, the final list comprised 2864 YSOs

(2562 with constructed SEDs and 302 YSOs in the saturated regions). The mass range of the YSOs is from 1.5 to 24 $M_{\odot}$.

Figure 3 shows the distribution of the selected YSOs in the two star-forming regions, with Class I and Class II objects shown by filled red and blue circles, respectively. Excluding the regions in the vicinity of the IRAS sources, all types of stellar objects are distributed relatively homogeneously in the molecular cloud. Additionally, in the UC HII regions, close to the IRAS sources, the selected YSOs form relatively dense concentrations or clusters. The evolutionary age spread of the vast majority of stellar objects in the IRAS clusters is small; from ∼1 to 7 Myr. Furthermore, the members of the IRAS clusters are more developed than the non-cluster objects.

The distribution of stellar population within the two star-forming regions on K versus J–K colour-magnitude diagram also shows certain different between the IRAS clusters and non-cluster regions. An overwhelming majority (more than 80%) of the non-cluster objects are younger then 0.1 Myr. In contrast, objects in the IRAS clusters are concentrated around the ZAMS.

5. Discussion and Conclusion

The search for and study of the young stellar population of the G045.49+00.04 and G045.14+00.14 star-forming regions located in the GRSMC 45.46+0.05 molecular cloud made it possible to obtain the following results:

- We obtained relatively robust parameters for 2562 YSOs with $\chi^2 < 100$. We also identified 302 YSOs located in the MIR-saturated regions based only on the J, H, and K photometric data.
- The stellar distribution shows the existence of dense clusters in the vicinity of the IRAS sources. The non-cluster objects are uniformly distributed in the molecular cloud.
- The study of the stellar parameters from different samples (i.e. clusters and non-cluster) showed differences between the two populations.
- Around 75% of the YSOs in the IRAS clusters are older than 0.1 Myr isochrone and are concentrated around the ZAMS.
- More than 80% of the non-cluster objetcs are younger than 0.1 Myr isochrone.

Based on the results, we concluded that dense clusters were formed in the UC HII regions, which include high- and intermediate-mass stellar objects. The evolutionary ages of these stars, in most cases, are several million years. The small spread of evolutionary ages suggests that the clusters owe their origin to a triggering shock.

The distribution of the non-cluster objects in the molecular cloud implies that their origin cannot be explained by the activity of the embedded massive star(s) in the UC HII regions. We assume that these uniformly distributed objects are part of the young stellar population of the GRSMC 45.46+0.05 molecular cloud. To understand the tracers of their origins, it is necessary to investigate the star formation history of the GRSMC 45.46+0.05 star-forming region as a whole.

In the coming works, we plan to find the trigger of star formation in the whole molecular cloud as well as the properties of Interstellar medium to reconstruct the star formation history.

Acknowledgements

This work was made possible by a research grant number № 21AG-1C044 from Science Committee of Ministry of Education, Science, Culture and Sports RA.

References

Azatyan N. M., 2019, Astron. Astrophys. , 622, A38

Azatyan N., Nikoghosyan E., Harutyunian H., Baghdasaryan D., Andreasyan D., 2022, Proc. Astron. Soc. Aust. , 39, e024

Bessell M. S., Brett J. M., 1988, Publ. Astron. Soc. Pac. , 100, 1134

Carpenter J. M., 2001, Astron. J. , 121, 2851

Churchwell E., 2002, Ann. Rev. Astron. Astrophys. , 40, 27

Churchwell E., et al., 2009, Publ. Astron. Soc. Pac. , 121, 213

Elmegreen B. G., Lada C. J., 1977, Astrophys. J. , 214, 725

Fazio G. G., et al., 2004, Astrophys. J. Suppl. Ser. , 154, 10

Flaherty K. M., Pipher J. L., Megeath S. T., Winston E. M., Gutermuth R. A., Muzerolle J., Allen L. E., Fazio G. G., 2007, Astrophys. J. , 663, 1069

Griffin M. J., et al., 2010, Astron. Astrophys. , 518, L3

Gutermuth R. A., et al., 2008, Astrophys. J. , 674, 336

Hartmann L., 2009, Accretion Processes in Star Formation: Second Edition. Cambridge University Press

Hernández J., Calvet N., Hartmann L., Briceño C., Sicilia-Aguilar A., Berlind P., 2005, Astron. J. , 129, 856

Keto E., 2007, Astrophys. J. , 666, 976

Lada C. J., Adams F. C., 1992, Astrophys. J. , 393, 278

Lada C. J., Lada E. A., 2003, Ann. Rev. Astron. Astrophys. , 41, 57

Lucas P. W., et al., 2008, Mon. Not. R. Astron. Soc. , 391, 136

McKee C. F., Tan J. C., 2003, Astrophys. J. , 585, 850

Meyer M. R., Calvet N., Hillenbrand L. A., 1997, Astron. J. , 114, 288

Molinari S., et al., 2016, Astron. Astrophys. , 591, A149

Peters T., Banerjee R., Klessen R. S., Mac Low M.-M., Galván-Madrid R., Keto E. R., 2010, Astrophys. J. , 711, 1017

Pilbratt G. L., et al., 2010, Astron. Astrophys. , 518, L1

Poglitsch A., et al., 2010, Astron. Astrophys. , 518, L2

Rieke G. H., Lebofsky M. J., 1985, Astrophys. J. , 288, 618

Robitaille T. P., Whitney B. A., Indebetouw R., Wood K., 2007, Astrophys. J. Suppl. Ser. , 169, 328

Schlegel D. J., Finkbeiner D. P., Davis M., 1998, Astrophys. J. , 500, 525

Simon R., Jackson J. M., Clemens D. P., Bania T. M., Heyer M. H., 2001, Astrophys. J. , 551, 747

Wright E. L., et al., 2010, Astron. J. , 140, 1868

Wu Y. W., et al., 2019, Astrophys. J. , 874, 94

Zinnecker H., McCaughrean M. J., Wilking B. A., 1993, in Levy E. H., Lunine J. I., eds, Protostars and Planets III. pp 429–495